



## **Performance Evaluation of LiBr-H<sub>2</sub>O Vapours Absorption System for an Office Building Cooling**

**Abhishek Ajay<sup>1\*</sup>, R. S. Gill<sup>2</sup> and Rupinder Pal Singh<sup>2</sup>**

<sup>1</sup>*Punjab Agricultural University, Ludhiana, 141004, India.*

<sup>2</sup>*Department of Mechanical Engineering, Punjab Agricultural University, Ludhiana, 141004, India.*

### **Authors' contributions**

*This work was carried out in collaboration among all authors. Author AA designed the study, wrote the protocol and wrote the first draft of the manuscript. Authors AA and RPS managed the literature searches. Authors AA and RSG managed the analyses of the study.*

### **Article Information**

DOI: 10.9734/AIR/2020/v21i730215

#### Editor(s):

(1) Dr. Slawomir Borek, Adam Mickiewicz University, Poland.

#### Reviewers:

(1) Qasim S. Mahdi, Mustansiriyah University, Iraq.

(2) Andrianaharinjaka Finiavana Aro-Zo Rakotonirina, University of Antsirananana, Madagascar.

Complete Peer review History: <http://www.sdiarticle4.com/review-history/58135>

**Original Research Article**

**Received 08 April 2020**

**Accepted 13 June 2020**

**Published 24 June 2020**

### **ABSTRACT**

The aim of this paper is to assess the energy performance by simulation of a single effect LiBr-H<sub>2</sub>O vapour absorption system for office room cooling under Ludhiana (31°N) climate conditions. In an absorption cooling system, compressor which is using high grade energy, replaced by a combination of generator and absorber. The low grade heat is supplied to the generator which produces the cooling effect in the evaporator section. In the present work, lithium bromide is used as absorbent and water as refrigerant. A thermodynamic simulation of the cycle is carried out to investigate the effects of office room temperature and condenser temperature on the performance of the LiBr-H<sub>2</sub>O vapour absorption system. It was concluded that coefficient of performance (COP) increases from 0.55 to 0.75 as office room temperature increases from 22 to 30°C for fixed value of condenser temperature of 46°C. The maximum COP was observed when system runs on least value of condenser temperature.

**Keywords:** Absorption refrigeration; LiBr-H<sub>2</sub>O; simulation; coefficient of performance; room cooling.

\*Corresponding author: E-mail: [abhirahul2811@gmail.com](mailto:abhirahul2811@gmail.com);

## 1. INTRODUCTION

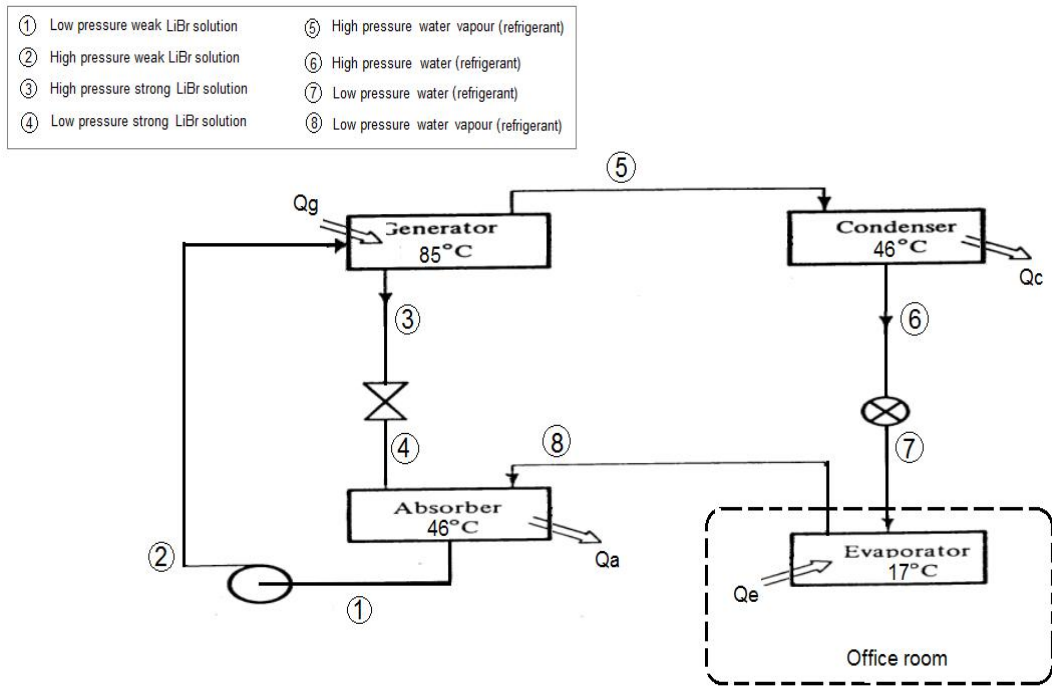
Refrigeration and air-conditioning requirement, either for cooling of household, offices, hotels, laboratories or public buildings or preservation and chilling purposes of perishable items, are increasing considerably day by day. The conventional refrigeration and air-conditioning systems, known as the vapor-compression refrigeration process (VCRC), is most widely used today to meet these refrigeration and cooling demands. However, it is well-known that the vapor-compression systems are using ozone depleting refrigerants which is responsible for causing global warming and other environmental issues [1,2]. Research and development of Absorption refrigeration machine reported in many research papers is a suitable option to resolve the above challenges [3]. The vapour absorption refrigeration cycle (VARC) runs on thermal energy with small electrical energy requirement compared with VCRC [4]. The thermal requirement of the VARC system can be fulfilled by low-cost sources such as biomass [5], solar [6,7], exhaust heat from engines [8,9] and waste heat from industrial processes [10]. The principle of working of a VARS is similar to that of a vapor compression system. In an absorption cooling system, low grade heat from any source is supplied in the generator section. The heat evaporates the refrigerant which is further expanded to produce cooling effect. The compressor of the vapor compression system is replaced with generator-absorber combination. The significant feature of the absorption system is to use thermal energy in comparison with the high grade electrical energy. In absorption cooling cycle, Lithium bromide (LiBr) is the most common absorbent with H<sub>2</sub>O as the refrigerant and in smaller absorption chillers rarely H<sub>2</sub>O is used as the absorbent and NH<sub>3</sub> as the refrigerant. However, LiBr has a very high affinity for H<sub>2</sub>O and in addition, H<sub>2</sub>O of course is relatively inexpensive and non-toxic [11]. Absorption cooling was invented by the French scientist Ferdinand Carré in 1858 [12]. Solar energy constitutes a popular application of absorption refrigeration which is free, zero emission as well as a clean energy source. Pohl et al. [13], Grossman and Zaltash [14], Sumathy et al. [15], Asdrubali and Grignaffini [16], Hiebler et al. [17], Gogoi and Talukdar [18], Konwar and Gogoi [19] and Kanti Deand Ganguly [20] and many others studied the performances of absorption refrigeration processes using LiBr/H<sub>2</sub>O as absorbant-refrigerant. According to the author's knowledge from review on vapour

absorption refrigeration system, the very minimum effort has been done on thermodynamic analysis of a vapour absorption air-conditioning system for office room cooling for different room temperature settings as per requirement of different comfort level of different persons. Keeping this in view, this study investigates the performance of LiBr–H<sub>2</sub>O based absorption refrigeration system for office room cooling under climate conditions of Ludhiana (31°N) to produce scientific results. The steady state mathematical model was formulated to investigate the effect of different office room temperature settings on coefficient of performance, circulation ratio, thermal load, concentration, system pressure and mass flow rate. In addition, the developed model can easily be extended to include different refrigerant-absorbent pairs for evaluating the thermal performance of single effect absorption cooling system.

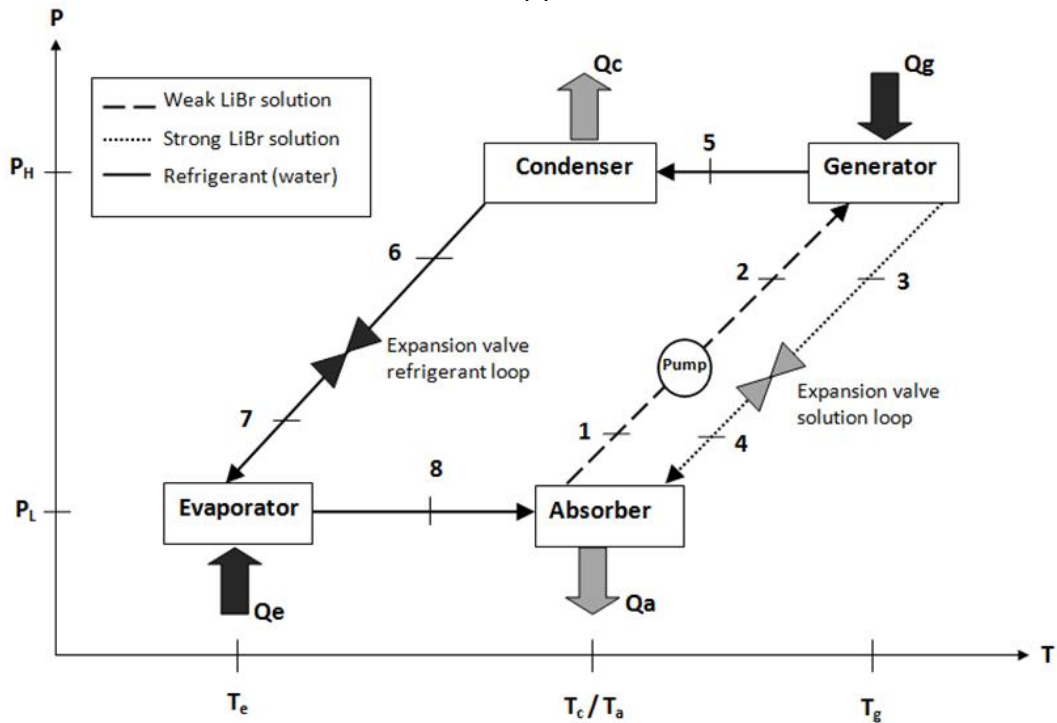
## 2. MATERIALS AND METHODS

### 2.1 System Description

In this work, the evaporator of LiBr–H<sub>2</sub>O absorption based refrigeration system is kept inside the office room to be cooled as shown in Fig. 1(a). In the LiBr–H<sub>2</sub>O absorption refrigeration system, LiBr is used as an absorbent and H<sub>2</sub>O as refrigerant. The H<sub>2</sub>O (liquid refrigerant) coming from the throttling valve (State 7) evaporates by absorbing the heat (Q<sub>e</sub>) from the office room (State 8). The refrigerant vapor coming from evaporator is absorbed and condensed into the LiBr–H<sub>2</sub>O solution coming from the expansion valve of solution loop i.e. weak in water percentage at state point 4, resulting in weak LiBr–H<sub>2</sub>O solution at state point 1. The heat produced (Q<sub>a</sub>) in absorber is rejected by cooling media. At state 1, the low pressure (P<sub>L</sub>) LiBr–H<sub>2</sub>O solution is pressurized by the solution pump to high pressure (P<sub>H</sub>) solution (State 2) and pump it into generator. In the generator, heat (Q<sub>g</sub>) is supplied to weak LiBr–H<sub>2</sub>O solution at high temperature to extract the refrigerant vapors and rich solution of absorbent returns back to the absorber. The vapor in superheated form condensed and rejected heat (Q<sub>c</sub>) in the condenser (state 6). Finally, condensed water (state 6) is throttled through expansion valve to low pressure (state 7). Fig. 1 (b) also illustrates the main components of a single-stage absorption refrigeration cycle represented in a pressure-temperature plot.



(a)



$Q_c$  - Heat rejected by condenser     $Q_g$  - Heat absorbed by generator     $Q_e$  - Heat absorbed by evaporator  
 $Q_a$  - Heat rejected by absorber

(b)

Fig. 1. (a) Schematic (b) P-T diagram of a absorption refrigeration system with different components

## 2.2 Mathematical Modeling

### 2.2.1 Model assumptions

In order to conduct the theoretical analysis of vapour absorption refrigeration cycle, the following basic assumptions have been made.

- Steady state processes.
- The outside air is considered as thermal reservoir and its temperature ( $T_o$ ) is taken as 40°C (constant) for the month of June at Ludhiana (31°N).
- The refrigerant-absorbent are assumed to be ideal.
- No pressure drop in system except throttling valves.
- Saturated condition at the exit of condenser and evaporator.
- Pump is isentropic and its efficiency is set at a constant value  $\eta_p = 50\%$ .
- The generator temperature ( $T_g$ ) is taken as 85°C (constant).

### 2.2.2 Thermodynamic formulations

The thermal analysis depends on the governing equation of first law of thermodynamics in each component of the cycle. For this, the mass and energy balance equations in steady state processes for the different parts of the refrigerating cycle with respect to Fig. 1 are established as follows [21]:

#### Evaporator

Heat absorbed in evaporator,  $Q_e = m_8 h_8 - m_7 h_7$  (Watts) (1)

#### Condenser

Heat rejection from condenser,  $Q_c = m_5 h_5 - m_6 h_6$  (Watts) (2)

#### Absorber

Heat rejection from absorber,  $Q_a = m_8 h_8 + m_4 h_4 - m_1 h_1$  (Watts) (3)

Mass balance,  $m_4 + m_8 = m_1$  (Total mass) (4)

$m_4 C_4 + m_8 C_8 = m_1 C_1$  (Mass of LiBr) (5)

#### Generator

Heat added to generator,  $Q_g = m_5 h_5 + m_3 h_3 - m_2 h_2$  (Watts) (6)

Mass balance,  $m_3 + m_5 = m_2$  (Total mass) (7)

$m_3 C_3 + m_5 C_5 = m_2 C_2$  (Mass of LiBr) (8)

### Efficiency of solution pump

$$\eta_p = \frac{1}{\rho_1} \frac{P_1 - P_2}{h_2 - h_1} \quad (9)$$

The absorption system uses the phenomenon of chemical absorption and generation of the refrigerant. The heat to the generator can be applied from solar, geothermal, waste heat or natural gas to vaporizes the refrigerant. The refrigerant vapors are cooled in the condenser and further expanded to produce the chilled effect inside the evaporator. Only a small fraction of electrical energy required to run the solution pumps. Hence, the COP of the absorption system is defined as follows:

$$COP = \frac{Q_e}{Q_g} \quad (10)$$

## 2.3 Calculation Procedure of Vapour Absorption Refrigeration for Office Room Cooling

A computer program is developed in QBasic language for the simulation of vapour absorption refrigeration system. The program is constructed to allow for a sequential computation of all the governing equation of the absorption system given in section 2.2.2. The thermodynamic and transport properties of water, required to solve the mass and energy balances of the mathematical model, are obtained from thermodynamic property correlation developed by Harr et al. [22], valid up to a pressure of 815 bar. Meanwhile, for LiBr-H<sub>2</sub>O solution, the following equations obtained by Patek and Klomfar [23], valid for full composition rate and from 273 to 500 K are used.

$$x = \frac{w/M_{LiBr}}{w/M_{LiBr} + (1-w)M_w} \quad (11)$$

$$P = \frac{1}{xM_{LiBr} + (1-x)M_w} \times \left[ T - \sum_{i=1}^8 a_i x^{m_i} (0.4 - x)^{n_i} \left( \frac{T}{T_c} \right)^{t_i} \right] \quad (12)$$

$$h = \frac{1}{xM_{LiBr} + (1-x)M_w} \times \left[ (1-x)h_f - h_c \sum_{i=1}^{30} a_i x^{m_i} (0.4 - x)^{n_i} T^{t_i} - T O t_i \right] \quad (13)$$

$$\rho = \frac{1}{xM_{LiBr} + (1-x)M_w} \times \left[ (1-x)\rho_f - \sum_{i=1}^2 a_i x^{m_i} \left( \frac{T}{T_c} \right)^{t_i} \right] \quad (14)$$

For the thermal analysis of the system, different operating parameter such as of the evaporator

temperature, condenser and absorber temperature are varied and the COP, mass flow rate, circulation ratio, concentration, system pressure and thermal load of the system is plotted. The input value of different operating parameters is given in Table 1. In this table, the five values of room temperature ( $T_r$ ) are considered as per comfort level for different persons and the temperature in evaporator ( $T_e$ ) is considered  $5^\circ\text{C}$  less than room temperature based on efficient fan-coil evaporator [21]. Based on different designs of heat exchanger, the condenser and absorber temperature having 4, 6, 8 and  $10^\circ\text{C}$  higher than outside air temperature of  $40^\circ\text{C}$  are studied. The condenser and absorber temperature are assumed to be same for each set of operating condition for this study.

### 2.4 Cooling Load Calculation

The different heating loads that must be rejected from the space to maintain temperature of room air ( $T_r$ ) at stable level as given in Fig. 2. Cooling load calculations is performed for an office room at Ludhiana ( $31^\circ\text{N}$ ). The dimension of this office

room is about 10 m (E-W)  $\times$  5 m  $\times$  4 m high. The walls of room have 250 mm thick brick with 10 mm thick layer of cement on it. The ceiling of room has 0.15 m thick concrete. North and south wall have two windows of 1 m  $\times$  1.5 m wide having glass panes 6 mm thickness. In this room, there is one officer, one computer operator, two attendants, one receptionist, four visitors, one 500W fridge, one 300 W photocopier machine, two fans of 100W each, six tube rods of 40W each. As the temperature difference between the room air and the ambient is the major parameter for the cooling load calculation therefore, for this study, the maximum outdoor air temperature ( $T_o$ ) of  $40^\circ\text{C}$  for the month of June at Ludhiana ( $^\circ\text{N}$ ) and inside room air temperature ( $T_r$ ) of 22, 24, 26, 28 and  $30^\circ\text{C}$  (Table 1) are considered. The sample calculation of different heat loads on office room for outdoor air temperature of  $40^\circ\text{C}$  and inside room air temperature of  $22^\circ\text{C}$ , for cooling load calculation, is given in Appendix [24]. The cooling load of the room for different inside room air temperature of 30, 28, 26, 24 and  $22^\circ\text{C}$  comes out to be as 17, 20, 23, 26 and 29 kW respectively.

**Table 1. The input data of different parameters**

Sr. No.	Parameter	Symbol	Temperature ( $^\circ\text{C}$ )
1.	Room / Evaporator temperature	$T_r/T_e$	22/17, 24/19, 26/21, 28/23, 30/25
2.	Absorber and condenser temperature	$T_c = T_a$	44, 46, 48, 50

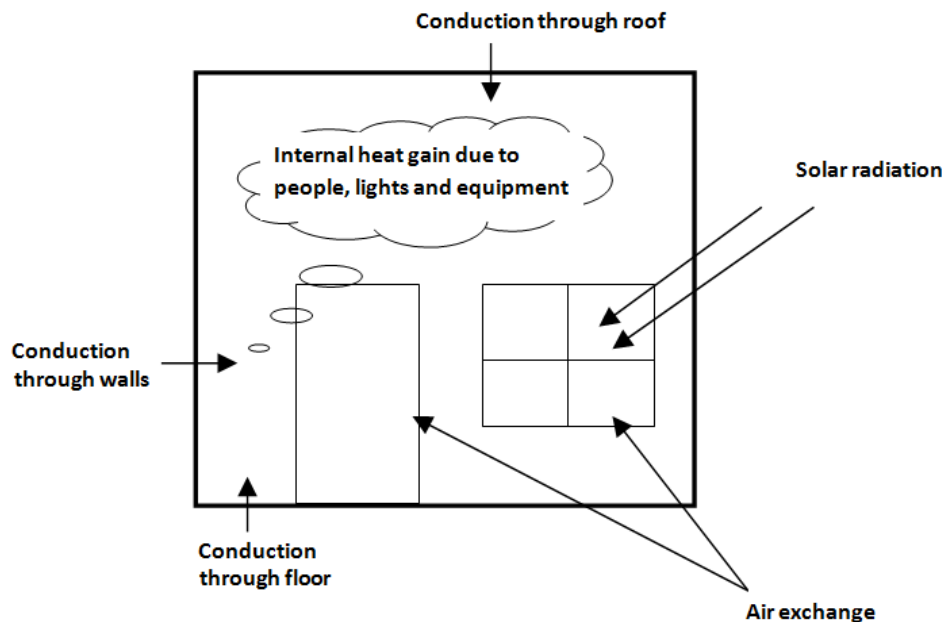


**Fig. 2. Different heat loads on office room for cooling load calculation**

### 3. RESULTS AND DISCUSSION

The results of parametric study of LiBr–H<sub>2</sub>O based absorption refrigeration cycles to provide air conditioning for summer is presented in this section. Table 2 shows the thermodynamic properties at various state points and energy flows to and from each component of vapour refrigeration system in reference to one set of operating conditions as shown below.

#### Input data

Room air temperature,  $T_r = 22^\circ\text{C}$   
 evaporator temperature,  $T_e = 17^\circ\text{C}$ ,  
 cooling load,  $Q_e = 29 \text{ kW}$ ,  
 absorber temperature,  $T_a = T_c = 46^\circ\text{C}$  and  
 outside air temperature,  $T_o = 40^\circ\text{C}$ .

The variation of COP increases from 0.55 to 0.75 (Fig. 3) as office room temperature is increased from 22 to 30°C (i.e. increase in evaporator temperature from 17 to 25°C), for fixed value of absorber and Condenser temperature of 46°C. This is because of decrease in CR value 19.79 to 7.0 as can be seen in Fig. 4 and increase in  $T_e$  from 17 to 25°C. Manu and Chandrashekar [25] also showed the increase in COP as CR decreases. Similar trend of increase in COP with increase in office room temperature can be observed for other values of absorber and Condenser temperatures. The best COP value of 0.78 is obtained with least value of absorber temperature ( $T_a$ ) and condenser temperature ( $T_c$ ) considered in this study.

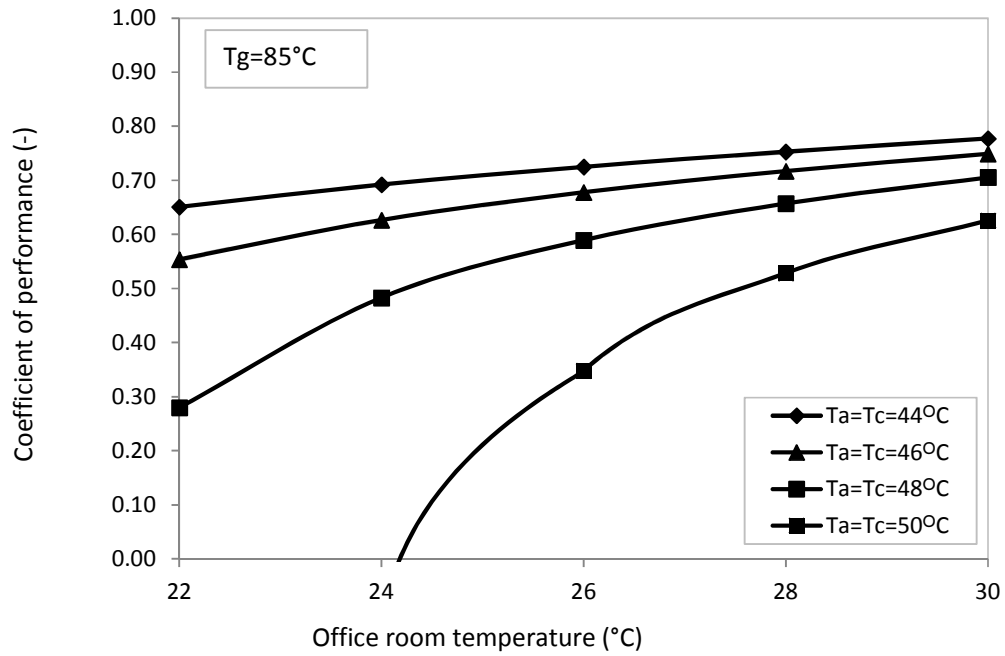
Fig. 5 presents the heat load variations on the office room temperature for fixed value of

absorber and Condenser temperature of 46°C and generator temperature of 85°C. It can be seen from Fig. 5 that when office room temperature increases from 22 to 30°C (i.e. increase in evaporator temperature from 17 to 25°C), there is a decrease in generator load ( $Q_g$ ) from 52.36 to 22.7 kW, absorber load ( $Q_a$ ) from 50.8 to 21.89 kW, condenser load ( $Q_c$ ) from 30.57 to 17.81 kW and pump work ( $W_p$ ) from 2.5 to 0.47 W (Fig 7). This decrease in thermal loads i.e.  $Q_g$ ,  $Q_a$  and  $Q_c$  and pump work ( $W_p$ ) is due to decreases in CR [25]. Aphornratana and Sriveerakul [26] also verified experimentally that,  $Q_g$ ,  $Q_a$  and  $Q_c$  decrease as circulation ratio (CR) decreases. It can be also seen from Fig. 5 that cooling load ( $Q_e$ ) on evaporative decreases with the increase in office room temperature which is due to decrease in the temperature difference of room and outside air ( $\Delta T$ ).

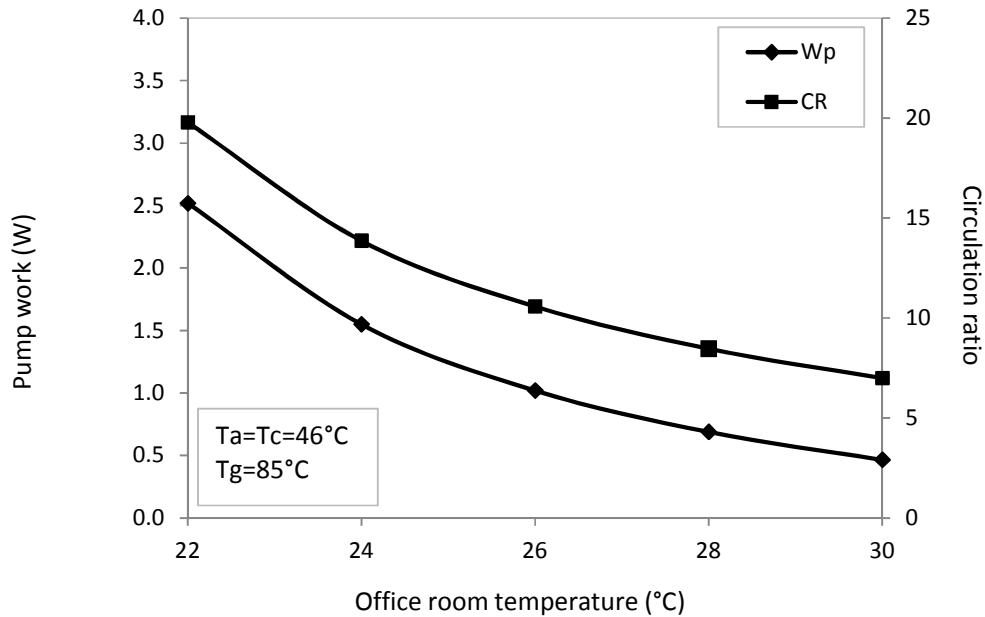
Fig. 6 demonstrates variations of the pressure as a function of office room temperature for constant absorber and Condenser temperature of 46°C and constant generator temperature of 85°C. As office room temperature increases from 22 to 30°C, there is an increase in low pressure side of the system, i.e. evaporator and absorber pressure, from 0.019 to 0.032 bar. This is well known fact that as saturation temperature increases saturation pressure also increases. However, there is no effect on high pressure side of the system, i.e. pressure in condenser and generator pressure remains constant at 0.101 bar. This is due to constant condenser temperature of 46°C. Manu and Chandrashekar [25] showed the similar findings.

**Table 2. The output data corresponding to one set of operating conditions**

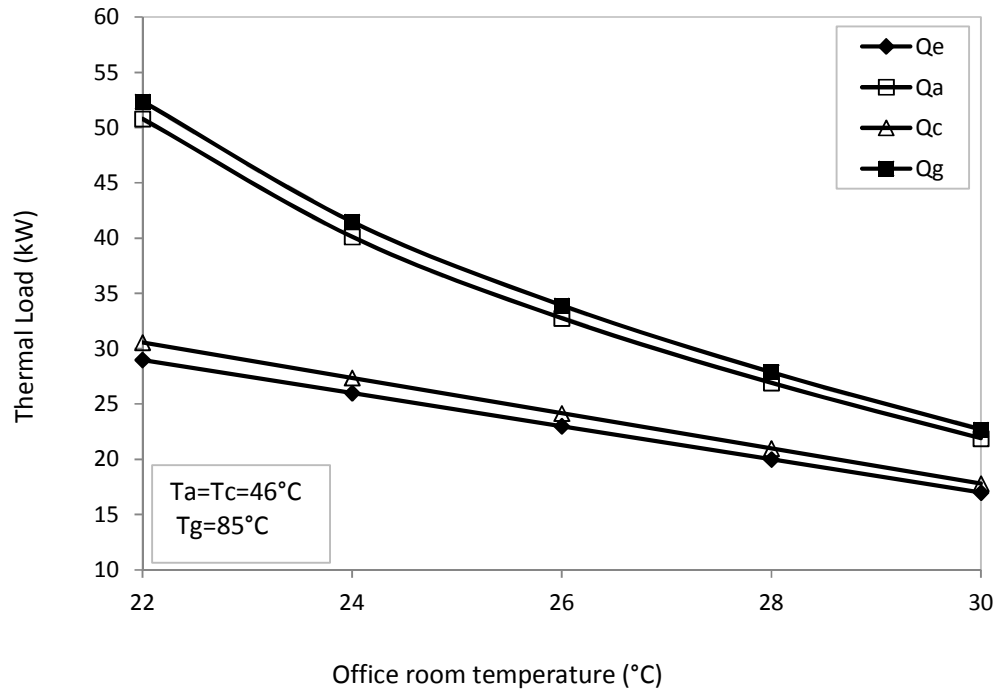
State point	Hi (kJ/kg)	Mi (g/s)	Pi (bar)	Ti (°C)	Wi (%)
1	103.2	245.3	0.019	46	53.9
2	103.2	245.3	0.101	46.7	53.9
3	192	232.9	0.101	85	56.7
4	192	232.9	0.101	73.3	56.7
5	2658	12.4	0.101	85	0.00
6	192.6	12.4	0.101	46	0.00
7	192.6	12.4	0.019	17	0.00
8	2532	12.4	0.019	17	0.00
Coefficient of performance,	COP	=		0.55 (-)	
Circulation ratio,	CR	=		19.79 (-)	
Heat rejected by absorber,	Qa	=		50.8 kW	
Heat rejected by condenser,	Qc	=		30.57 kW	
Heat absorbed by evaporator,	Qe	=		29.0 kW	
Heat absorbed by generator,	Qg	=		52.36 kW	
Solution pump work,	Wp	=		2.518 W	



**Fig. 3. Variation of coefficient of performance with the office room temperature**  
*Ta – Absorber temperature, Tc – Condenser temperature, Tg – Generator temperature*

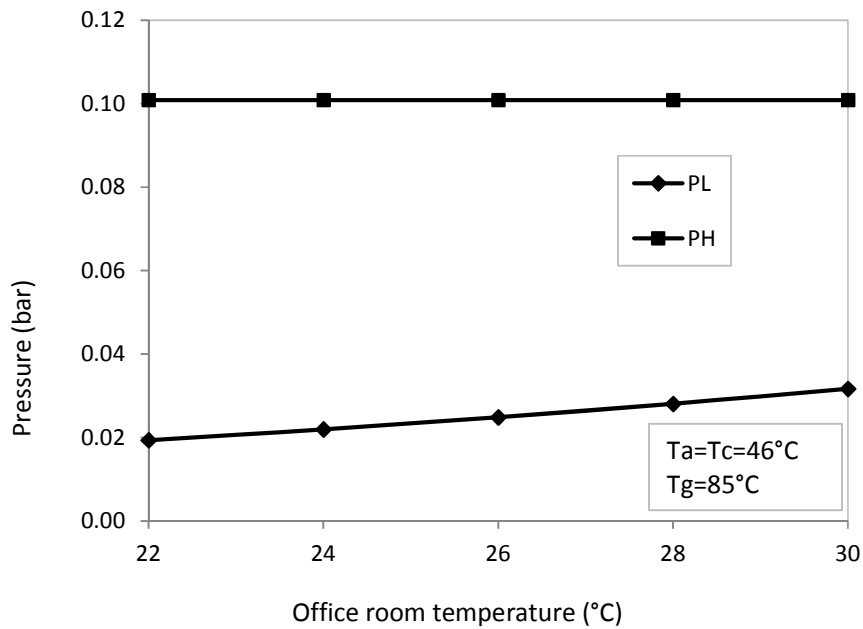


**Fig. 4. Variation of concentration ratio and solution pump work with the office room temperature**  
*Ta – Absorber temperature, Tc – Condenser temperature, Tg – Generator temperature, Wp – Solution pump work, CR – Circulation ratio*



**Fig. 5. Variation of thermal load with the office room temperature**

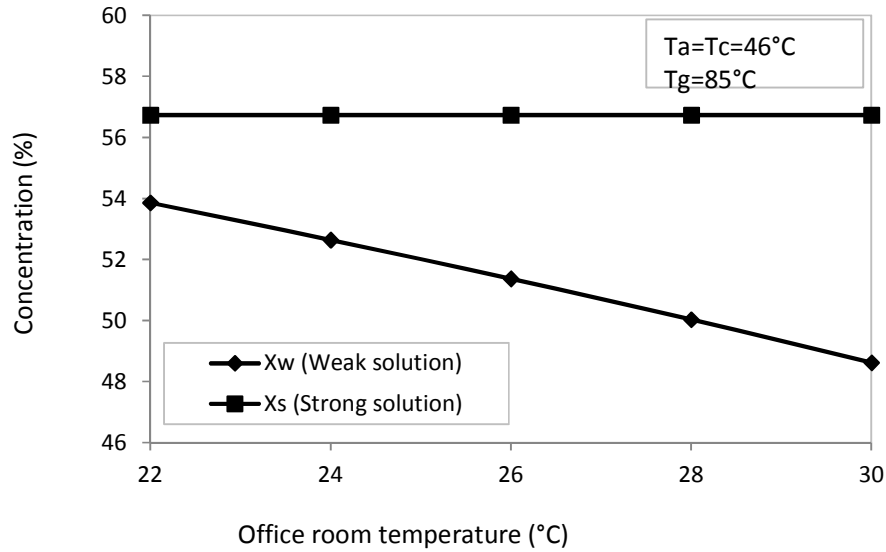
$T_a$  – Absorber temperature,  $T_c$  – Condenser temperature,  $T_g$  – Generator temperature,  $Q_e$  – Heat absorber in evaporator,  $Q_a$  – Heat rejected in absorber,  $Q_c$  – Heat rejected in condenser,  $Q_g$  – Heat absorbed in generator



**Fig. 6. Variation of pressure with the office room temperature**

$T_a$  – Absorber temperature,  $T_c$  – Condenser temperature,  $T_g$  – Generator temperature,  $P_L$  – Low pressure,  $P_H$  – High pressure

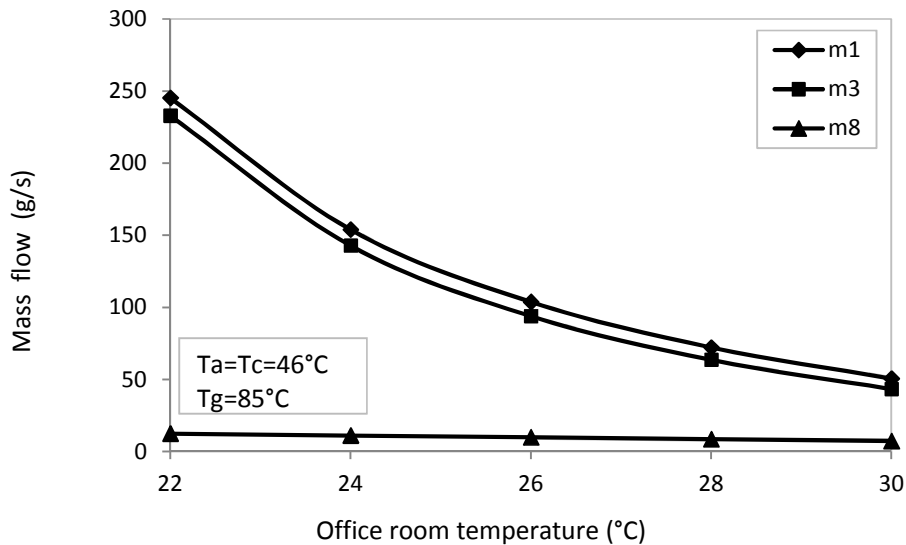




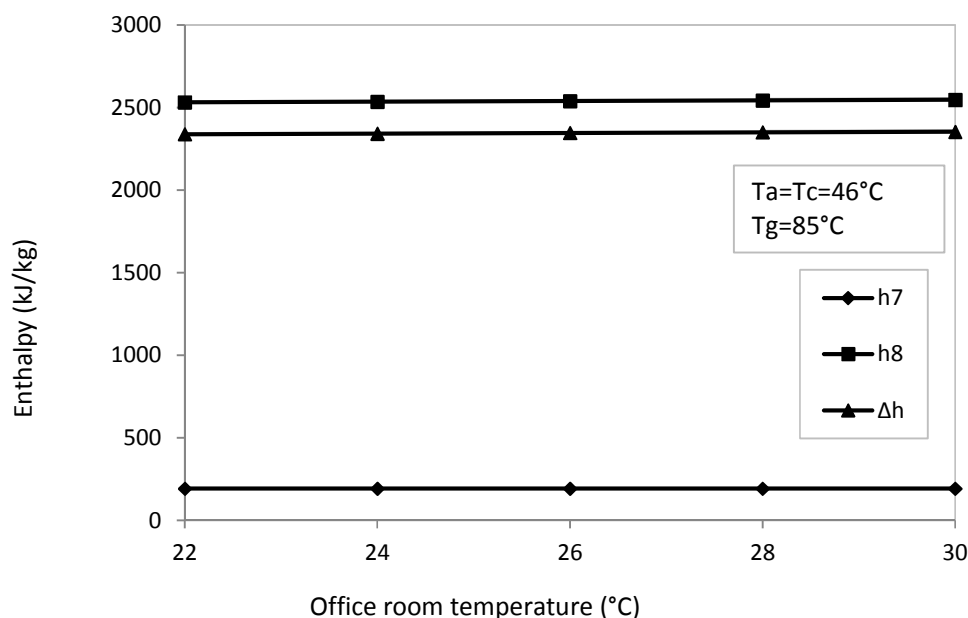
**Fig. 7. Variation of concentration with the office room temperature**  
*T<sub>a</sub>* – Absorber temperature, *T<sub>c</sub>* – Condenser temperature, *T<sub>g</sub>* – Generator temperature

Fig. 7 shows the concentration as a function of office room temperature for fixed absorber temperature and condenser temperature of 46°C and fixed generator temperature of 85°C. The decrease in concentration (53.86 to 48.62%) of weak solution ( $w_1$ ) leaving absorber with increase in office room temperature is observed. This decrease in concentration is due to an increase in weak solution pressure ( $P_L$ ) with the increase

in office room temperature (Fig. 6). However, the concentration of strong solution coming out of the generator remain constant ( $w_1 = 56.73\%$ ), this is due to a constant pressure of strong solution ( $P_H$ ) coming out of the generator for all values of office temperatures (Fig. 6). The results of Fig. 7 are in accordance with the results presented in the references [25,27].



**Fig. 8. Variation of mass flow with office room temperature**  
*T<sub>a</sub>* – Absorber temperature, *T<sub>c</sub>* – Condenser temperature, *T<sub>g</sub>* – Generator temperature, *m<sub>1</sub>* - mass flow rate of weak solution, *m<sub>3</sub>* - mass flow rate of strong solution, *m<sub>8</sub>* - mass flow rate of refrigerant in evaporator



**Fig. 9. Variation of enthalpy with office room temperature**

$T_a$  – Absorber temperature,  $T_c$  – Condenser temperature,  $T_g$  – Generator temperature,  
 $\Delta h = (h_8 - h_7)$  – enthalpy of evaporation

Fig. 8 shows of mass flow rate variations with room temperature at constant absorber and condenser temperature of 46°C and constant generator temperature of 85°C. As office room temperature increases, the decrease in weak solution mass flow rates ( $m_1$ ) from 245.3 to 50.51 g/s, decrease in strong solution mass flow rates ( $m_3$ ) from 232.9 to 43.29 g/s observed which is because of decrease in CR (Fig. 4). It is also observed decrease in refrigerant mass flow rate ( $m_8$ ) in evaporator from 12.4 to 7.223 g/s. This is because with an increase in the  $T_e$  from 22 to 30°C, the cooling load on evaporator ( $Q_e$ ) decreases (Fig. 5) and enthalpy of evaporation ( $\Delta h = h_8 - h_7$ ) in evaporator increases (Fig. 9), resulting in a decrease in mass flow rate ( $m_8$ ) through evaporator as given by equation (3). The results of Fig. 8 are in line with the other studies [25,28].

#### 4. CONCLUSION

In this study, a simulation of the single-stage LiBr–H<sub>2</sub>O vapor absorption refrigeration system (VARS) for an office room cooling was done and the system performances were analyzed. This VARS is alternative to conventional VCRS. In this system, LiBr has been opted as absorbent and H<sub>2</sub>O as

refrigerant for cooling purpose. The results revealed that the COP rises from 0.5538 to 0.7489 with 22 C to 30°C increase in room temperature for fixed value of absorber and condenser temperature of 46°C. The best COP is attained with least value of condenser and absorber temperature. Further, the CR value of the system showed its significance in deciding the performance of the system. Using computer program developed in QBASIC language for thermodynamic analysis of LiBr–H<sub>2</sub>O vapor absorption refrigeration system, the effect of office room conditions on coefficient of performance, circulation ratio, thermal load, concentration, system pressure and mass flow rate can be evaluated with higher degree of accuracy and faster rate

#### ACKNOWLEDGEMENTS

The authors thank the Mechanical Engineering Department, College of Agricultural Engineering & Technology, Punjab Agricultural University, for its support and co-operation.

#### COMPETING INTERESTS

Authors have declared that no competing interests exist.

## REFERENCES

1. Venkatarathnam G, Murthy S. Refrigerants for vapour compression refrigeration systems Resonance. 2012;17:139–62.
2. Bhatkar VW, Kriplani VM, Awari GK. Alternative refrigerants in vapour compression refrigeration cycle for sustainable environment: A review of recent research. Int. J. Environ. Sci. Technol. 2013;10:871–880.
3. Nikbakhti Rasoul, Wang Xiaolin, Hussein Ahmed Kadhim, Iranmanesh Aghil. Absorption cooling systems – Review of various techniques for energy performance enhancement. Alexandria Engineering Journal. 2020;59(2):707-38.
4. Xiaohui She, Yin Yong-gao, Mengfei Xu, Xiaosong Z. A novel low-grade heat-driven absorption refrigeration system with LiCl-H<sub>2</sub>O and LiBr-H<sub>2</sub>O working pairs. International Journal of Refrigeration. 2015;58. DOI: 10.1016/j.ijrefrig.2015.06.016
5. Mbikan Munyeowaji, Al-Shemmeri Tarik. Computational model of a biomass driven absorption refrigeration system energies. 2017;10:234. DOI: 10.3390/en10020234
6. Konfe A, Kam S, Ousmane M, Bathiebo DJ. Comparative thermodynamic study of five couples used in solar cooling with adsorption by simulation. Current Journal of Applied Science and Technology. 2016; 17(2):1-17. Available: <https://doi.org/10.9734/BJAST/2016/28554>
7. Osman Wageiallah Mohammed, Guo Yanling. Comprehensive parametric study of a solar absorption refrigeration system to lower its cut in/off temperature. Energies. 2017;10:1746. DOI: 10.3390/en10111746
8. Sharif HZ, Leman AM, Muthuraman S, Mohd Najib Mohd Salleh, Supaat Zakaria. Performance analysis of single stage LiBr-water absorption machine operated by waste thermal energy of internal combustion engine: Case study, AIP Conference Proceedings. 1885;020210. Available: <https://doi.org/10.1063/1.5002404>
9. Kaewpradub Sorawit, Sanguanduean Prawit, Katesuwan Wattanapong, Chimres Nares, Punyasukhananda Phatthi, Godson Asirvatham Lazarus, Mahian Omid, Dalkilic Ahmet Selim, Wongwises Somchai. Absorption refrigeration system using engine exhaust gas as an energy source, Case Studies in Thermal Engineering. 2018;12:797-804.
10. Neave A. Heat pumps and their applications. In: Dennis A, editor. Snow, Plant Engineer's Reference Book. 2<sup>nd</sup> ed. Butterworth-Heinemann; 2002.
11. Shahad H, Hadi N. Overview of working pair used in absorption refrigeration technologies. International Journal for Research in Applied Science & Engineering Technology. 2018;6:662-678.
12. Lee RJ, Di Guilio RM, Jeter SM. Properties of lithium bromide–water solutions at high temperatures and concentration. II. Density and viscosity. ASHRAE Trans. 1990;96: 709–28.
13. Pohl JP, Hellmann HM, Grossman G. Investigation and comparison of two configurations of a novel open-cycle absorption chiller. International Journal of Refrigeration. 1998;21(2):142–49.
14. Grossman G, Zaltash A. ABSIM – Modular simulation of advanced absorption systems. International Journal of Refrigeration. 2001;24:531–43.
15. Sumathy K, Huang ZC, Li ZF. Solar absorption cooling with low grade heat source – A strategy of development in South China. Solar Energy. 2002;72(2): 155–65.
16. Asdrubali F, Grignaffini S. Experimental evaluation of the performances of a LiBr/H<sub>2</sub>O absorption refrigerator under different service conditions. International Journal of Refrigeration. 2005;28:489–97.
17. Hiebler S, Mehling H, Schweigler C, Helm M. 2008. Low temperature latent heat storage for a solar heating and cooling system –operational experience. In: World Renewable Energy Congress, Glasgow, UK. 2008;1759–1764.
18. Gogoi TK, Talukdar K. Thermodynamic analysis of a combined reheat regenerative thermal power plant and water–LiBr vapor absorption refrigeration system, Energy Conversion and Management. 2014;78: 595-610.
19. Konwar D, Gogoi TK. Performance of double effect H<sub>2</sub>O–LiCl absorption refrigeration systems and comparison with H<sub>2</sub>O–LiBr systems, Part 1: Energy analysis. Thermal Science and Engineering Progress. 2018;8:184-203.
20. De Ramen Kanti, Ganguly A. Performance comparison of solar-driven single and double-effect LiBr-water vapor absorption

- system based cold storage. Thermal Science and Engineering Progress. 2020; 17:100488.
21. Haar L, Gallagher JS, Kell GS. NBS/NRC steam tables Hemisphere Publishing Co.; 1984.
  22. Patek J, Klomfar J. A computationally effective formulation of the thermodynamic properties of LiBr-H<sub>2</sub>O from 273 to 500 K over full composition range. Int. J. of Refrigeration. 2006;29:566-78.
  23. Hundy GF, Trott AR, Welch TC. Refrigeration, air conditioning and heat pumps. 5<sup>th</sup> Edition; 2016.
  24. Bowman M, Debray SK, Peterson. Cengel. Heat and mass transfer, a practical approach. McGraw Hill; 1993.
  25. Manu S, Chandrashekar TK. A simulation study on performance evaluation of single-stage LiBr-H<sub>2</sub>O vapor absorption heat pump for chip cooling, International Journal of Sustainable Built Environment. 2016; 5(2):370-86.
  26. Aphornratana S, Sriveerakul T. Experimental studies of a single effect absorption refrigerator using aqueous lithium-bromide: Effect of operating condition to system performance. Exp. Therm Fluid Sci. 2007;32:658-69. Available: <http://dx.doi.org/10.1016/j.expthermflusci.2007.08.003>
  27. Chaudhari SK, Paranjape DV, Eisa MAR, Holland FA. A study of the operating characteristics of a Water-Lithium Bromide absorption heat pump. Heat Recovery Syst. 1985;5(4): 285-97. Available: [http://dx.doi.org/10.1016/0198-7593\(85\)90003-7](http://dx.doi.org/10.1016/0198-7593(85)90003-7).
  28. Florides GA, Kalogirou SA, Tassou SA, Wrobel LC. Design and construction of a LiBr-water absorption machine. Energy Convers. Manage. 2003;44:2483-508. Available: [http://dx.doi.org/10.1016/S0196-8904\(03\)00006-2](http://dx.doi.org/10.1016/S0196-8904(03)00006-2)

## APPENDIX

The heat load calculations for outdoor air temperature of 40°C and inside room air temperature of 22°C, i.e. air temperature difference between outside and room air of 18°C, are as under:

### a) Heat load due to conduction through roof, floor and walls

Heat gain through ceilings, floors, walls, and doors is due to temperature difference of air across them. The heat gain also depends upon the overall heat transfer coefficient of different components of room which further depend on thermal conductivity of material and heat transfer coefficient of outside and inside air of office room. The thermal conductivity of brick, cement, concrete, glass, wood is taken as 2.76, 1.56, 5.57, 3, 1.3 kJ/h-m-K respectively and the heat transfer coefficient of outside and inside air as 270 kJ/h-m<sup>2</sup>-K and 150 kJ/h-m<sup>2</sup>-K respectively. The overall heat transfer coefficient of different components of room is calculate as under

$$U_{\text{wall}} = 1/(1/h_o + t_{\text{brick}}/k_{\text{brick}} + t_{\text{cement}}/k_{\text{cement}} + 1/h_i) \\ = 1/(1/270 + 0.25/2.76 + 0.01/1.56 + 1/150) = 9.314 \text{ kJ/h-m}^2\text{-K}$$

$$U_{\text{door}} = 1/(1/270 + 0.04/1.3 + 1/150) = 24.31 \text{ kJ/h-m}^2\text{-K}$$

$$U_{\text{glass}} = 1/(1/270 + 0.006/3 + 1/150) = 80.838 \text{ kJ/h-m}^2\text{-K}$$

$$U_{\text{ceiling}} = 1/(1/270 + 0.15/5.57 + 1/150) = 26.81 \text{ kJ/h-m}^2\text{-K}$$

Heat gain through different parts of the building can be estimated by using following

$$Q_{\text{North}} = [(Ax U)_{\text{wall}} + (Ax U)_{\text{door}} + (Ax U)_{\text{window}}] (T_{o(\text{max})} - T_r) \\ = [(10 \times 4 - 2 \times 1 - 2 \times 1 \times 1.5) 9.314 + (2 \times 1) 24.31 + (2 \times 1 \times 1.5) 80.836] \times 18 \\ = 11104.8 \text{ kJ/h}$$

$$Q_{\text{South}} = [(Ax U)_{\text{wall}} + (Ax U)_{\text{window}}] (T_{o(\text{max})} - T_r) \\ = [(10 \times 4 - 2 \times 1 \times 1.5) 9.314 + (2 \times 1 \times 1.5) 80.836] \times 18 = 10568.8 \text{ kJ/h}$$

$$Q_{\text{East-West}} = (Ax U)_{\text{wall}} (T_{o(\text{max})} - T_r) \\ = [2(5 \times 4) 9.314] \times 18 = 6705.7 \text{ kJ/h}$$

$$Q_{\text{ceiling}} = (Ax U)_{\text{ceiling}} (T_{o(\text{max})} - T_r) \\ = [(10 \times 5) 26.81] \times 18 = 24124.2 \text{ kJ/h}$$

The total heat gain due to structure is therefore,

$$Q_{\text{structure}} = 11104.8 + 10568.8 + 6705.7 + 24124.2 = 52,506 \text{ kJ/h}$$

#### b) Heat load due to solar radiation

Considering solar heat gain load as 36% total heat gain load due to structure, the heat gain due to structure including solar radiation is given by

$$Q_{(\text{Structure} + \text{Solar rad.})} = 0.36 \times 52,506 = 18,902.16 \text{ kJ/h}$$

#### c) Heat load due to air exchange

Both sensible and latent heat is considered for the infiltration as entry of outside air into the conditioning area influences both the humidity and temperature level of air. The number of air changes/24 hours is assumed to be 4.99 for office volume of  $10 \times 5 \times 4 = 200 \text{ m}^3$ .

Therefore infiltration air =  $4.99 \times 200/24 = 41.6 \text{ m}^3/\text{h}$

Ventilation required for 8 persons in case of private office is:  $8 \times 12 \times 10^{-3} \times 3600 = 345.6 \text{ m}^3/\text{h}$

Therefore heat load based on total air exchange:  $(41.6 + 345.6) \times \rho_{\text{air}} \times c_p \times (T_o - T_i) = 387.2 \times (1.013/2872 \times 298) \times 1.004 (40 - 22) = 14599.4 \text{ kJ/h}$

#### d) Heat load due to internal heat gain

The primary sources of internal heat gain are equipments, occupants and lights operating within the cooling space.

(i) Heat load due to occupants =  $(2 \text{ clerk} \times 500) + (2 \text{ attendants} \times 600) + (4 \text{ persons} \times 450) + (1 \text{ receptionist} \times 600) = 4600 \text{ kJ/h}$

(ii) Heat load due to appliances =  $[(2 \text{ fans} \times 100) + (6 \text{ tubes} \times 40) + (1 \text{ photocopy machine} \times 300) + (1 \text{ refrigerator} \times 500)] \times 3600/1000 = 4464 \text{ kJ/h}$

Total heat load due to internal heat gain = Occupants Load + Appliances load =  $4600 + 4464 = 9064 \text{ kJ/h}$

The total Heat load =  $52,506 + 18,902.16 + 14599.4 + 9064 = 95071.5 \text{ kJ/h}$

Taking 10% safety factor, the total heat load on air conditioning apparatus is found to be:  $95071.5 \text{ kJ/h} \times 1.10 = 104578.7 \text{ kJ/h}$  or 29 kW

© 2020 Ajay et al.; This is an Open Access article distributed under the terms of the Creative Commons Attribution License (<http://creativecommons.org/licenses/by/4.0>), which permits unrestricted use, distribution, and reproduction in any medium, provided the original work is properly cited.

Peer-review history:  
The peer review history for this paper can be accessed here:  
<http://www.sdiarticle4.com/review-history/58135>